ORIGINAL ARTICLE

INTERNATIONAL JOURNAL OF RESEARCH IN PHARMACEUTICAL SCIENCES

Published by JK Welfare & Pharmascope Foundation Journal Home Page: www.ijrps.com

Synthesis and Characterization of Cadmium with Titanium Oxide (Cd-TiO_2) Nanocomposite: Testing its Antibacterial Effect

Daniel Sam N[1], Anish C I[1], Sabeena G[2], Rajaduraipandian S[3], Manobala[2], Annadurai G[*3], Jaya Rajan M[1]

[1]Annai Velankanni College, Tholayavattam – 629157, Kanniyakumari, Tamil Nadu, India
[2]Sri Paramakalyani Centre of Excellence in Environmental Sciences, Manonmaniam Sundaranar University, Alwarkurichi - 627412, Tirunelveli, Tamil Nadu, India
[3]Sri Paramakalyani College, Manonmaniam Sundaranar University, Alwarkurichi - 627412, Tirunelveli, Tamil Nadu, India

Article History:

Received on: 20 Aug 2021
Revised on: 25 Sep 2021
Accepted on: 27 Sep 2021

Keywords:

Cd-TiO2 Nanocomposite, Characterisation, Antibacterial Activity

ABSTRACT

Sol gel methods were used for the study of the antimicrobial activity of Cd-TiO_2 Nanocomposite against gram-negative and positive bacteria. These Cd-TiO_2 Nanocomposites have been characterized by various optical and electrochemical techniques. They have been exhibited by X-ray diffraction, scanning electron microscopy, ultraviolet spectroscopy, and infrared spectroscopy. The structures of the various XRD patterns indicate that the product has a rhombohedral structure. The particle size of Cd-TiO_2 nanocomposite is 35nm. The SEM images confirm the spherical appearance of the sample. The energy dispersive X-ray spectra have been confirmed as well and then C, O, Ti, Cd, Pt element are present in Cd-TiO_2 Nanocomposite. The weight percentage of Cadmium is 5.8%, Ti is 51.03%, C is 5.13% and O is 31.75% in Cd-TiO_2 Nanocomposite. BET image shows that the major pore size distribution of Cd-TiO_2 nanocomposites is ranged from 2.24 nm. The Cd-TiO_2 nanocomposite showed that the antibacterial activity when tested against the pathogens only gram-negative bacteria such as *Pseudomonas*. The zone of minimum inhibition concentration was measured in a range of 20mm in 25μl and 30mm in 100μl.

*Corresponding Author

Name: Annadurai G
Phone:
Email: gannadurai@msuniv.ac.in

ISSN: 0975-7538

DOI: https://doi.org/10.26452/ijrps.v12i4.4900

Production and Hosted by

IJRPS | www.ijrps.com

INTRODUCTION

The increasing number of applications of nanotechnology has led to the development of various synthetic materials with nanoscale properties (Giovanni *et al.*, 2015). Since ancient times, metals have been used as bactericidal agents. Many of these include gold, silver, titanium, chromium, manganese, and zinc (Vanaja *et al.*, 2013).

Cadmium nanocrystals have recently received a lot of attention due to their unique size dependent optical and electrical properties caused by the quantum confinement effect. Their properties can be fine-tuned by affixing them to various suitable materials, which are used for important technological purposes such as antibacterial activity (Li *et al.*, 2011; Demir *et al.*, 2012; Qian *et al.*, 2012).

Titanium dioxide has a wide range of crystalline structures that are used in solar cells, air purifier catalysts, photovoltaic materials, gas and humidity sensors, and antireflective coatings (Han *et al.*, 2006; Samuel *et al.*, 2005; Chen *et al.*, 2006). Powdered titanium oxide is also commonly used in toothpastes as a whitener (Malarkodi *et al.*, 2013). The antibacterial, antifungal, and antiviral activities of nanoparticles have been roughly investigated in comparison with other metals, but only a few authors have reported the antibacterial activity of metals such as cadmium nanocrystals in recent years (Zare *et al.*, 2018; Tabatabaee *et al.*, 2013). Because of their smaller size, highly optical fluorescence property, and ease of tissue functionalization, the development of novel cadmium-based quantum dots or carbon materials has enormous potential in the treatment and identification of cancer, as well as targeted drug delivery (Rzigalinski and Strobl, 2009). It has been reported that doping TiO_2 with various elements significantly improved its receptivity to visible light (Tsutomu *et al.*, 2003; Pelaez *et al.*, 2012). In recent years, there has been a growing interest in Cadmium-Titanium Oxide nanocomposite as a potential new material for optical fibre (Fades *et al.*, 1993; Dislich, 1993; Pettit *et al.*, 1993). To replace other materials, pure and high quality Cadmium with Titanium Oxide nanocomposite of good optical quality are required. In general, reaction sintering has been found to be difficult to control, especially when a chemically homogeneous, single phase product with high purity, high density, and uniform microstructure is desired. Sol-Gel processing has been investigated extensively as an alternative to conventional processing (Phani *et al.*, 1998). This method entails controlled hydrolysis of an alkoxide, followed by condensation, which results in the formation of a gel. The structure of the final compound or material is extremely sensitive to pH, reactant stability, water content, and impurities. We describe the synthesis of Cadmium with Titanium Oxide (Cd-TiO_2) nanocomposite powders using a Sol-Gel technique, which results in high purity crystalline powders at temperatures lower than solid state reactions. After proper morphological and structural characterization of the prepared sample using Scanning Electron Microscopy (SEM), Fourier Transform Infrared Spectroscopy (FTIR), Ultraviolet Spectroscopy (UV), and X-ray diffraction (XRD). We tested the prepared Cadmium with Titanium Oxide (Cd-TiO_2) nanocomposite against these bacteria to study its antibacterial effect against Gram-negative and Gram-positive bacteria.

MATERIALS AND METHODS

Chemicals and Materials

Sigma-Aldrich, Inc. provided titanium (IV) isopropoxide (TIP, 97.0 percent), N-dimethylformamide (DMF, 99.8 percent), and 1-butyl-3-methylimidazolium hexafluorophosphate (PF_6, 97.0 percent.(Milwaukee, WI).

In our experiments, we used 99.8 percent Cadmium Sulphate and 99.5 percent acetonitrile. All of these chemicals were used exactly as they were given to us. Except for the antibacterial tests, which used sterilised H_2O, all experiments used deionized water.

Preparation of Cd-TiO_2 Nanocomposite Powders

A solution was prepared with 5 mL of PF6 and 45 mL of DMF, in which the desired amount of $CdSO_4$ was dissolved. With vigorous stirring, titanium(IV) isopropoxide (9.68 mL) was slowly added to the solution. Dropwise additions of deionized H_2O (2.28 mL) were made to hydrolyze and form a gel. The gel was washed with acetonitrile repeatedly after overnight ageing to remove the entrapped PF_6, vacuum-dried at 80°C, and calcined in air at 600°C for 4 hours to produce Cd-TiO_2 nanocomposite powder.

Characterization of Cd-TiO_2 Nanocomposite

To analyse the chemical compositions of Cd-TiO2, the specific surface area (BET) was also determined. X-ray diffraction (XRD) patterns were recorded on a powder X-ray diffractometer (X'pert Pro) to study the crystalline structure. A Scanning Electron Microscope (SEM, Model JEOL JEM-2010F) was used in conjunction with an energy-dispersive X-ray spectroscopy (EDX) probe to examine the morphology of a Cd-TiO_2 Nanocomposite. The bonds and stretching modes were determined using a Fourier transform infrared (FTIR) spectrometer (BRUKER Vertex-70).

Antibacterial activity

The standard well diffusion method (Azam *et al.*, 2012) was used to test antibacterial susceptibility against gramme negative bacteria such as E. coli, Pseudomonas, and Enterobacter and gramme positive bacteria such as Staphylococcus aureus and Bacillus subtilis. Bacterial cultures were grown for 24 hours in Nutrient broth media. The wells were then filled with a constant volume of Cd-TiO_2 nanocomposite and water as a control. The plates were chilled for 5–10 minutes to allow for successive diffusion before the bacterial strains were incubated at 37°C for 24 hours. The diameter of the inhibition zone was measured and recorded after incubation. The experiments were carried out in triplicate.

RESULT AND DISCUSSION

X-ray Diffraction

For phase identification, X-ray diffraction (XRD) is used, and the diffracted intensities are recorded as a function of 2. Figure 1 depicts the XRD pattern of a Cd-TiO_2 nanocomposite powder calcined at 600°C for 4 hours. The specific diffraction peaks are shown in Figure 1 at 27.1°, 36.0°, 39.0°, 41.1°, 44.0°, 54.5°, 56.5°, 63.0°, 64.5°, and 69.0°. The crystalline size of the phase is indicated by all peaks of Cd-TiO_2 nanocomposite. Sharp and intense peaks, on the other hand, are observed for the sample that was calcined at 600°C for 4h indicating a higher degree of crystallinity in the pure TiO_2 sample, a weak (JCPDS No. 29-1360) peak was observed. Sharp peak represent as (Cd- TiO_2 nanocomposite) Cadmium present from Titanium Oxide nanopowder. For the sample of all the diffraction lines agree with reported values and match with the JCPDS data (card No: 29–277) confirming the formation of rhombohedral structure. The crystallite size is calculated and found to be Scherrer formula applied to the three highest peak such as 27.1°, 36.0°, 54.5° orientation which is the maximum reflection of the rhombohedral structure of Cd-TiO_2 nanocomposite. The particle size of Cd-TiO_2 nanocomposite in 35nm. The increased Cd loading appears to increase the size of the TiO2 crystallites in the powders. The size of the TiO_2 particles is expected to vary similarly (Phani *et al.*, 2000).

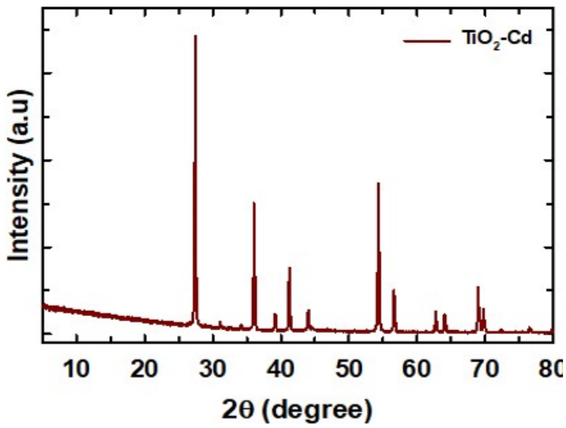

Figure 1: The XRD image of Cd-TiO_2 Nanocomposite

Ultra Violet Spectroscopy

Figure 2 shows that the exhibit UV-Vis spectrophotometer of synthesized Cd-TiO_2 nanocomposite powder by using solgel method. The Cd-TiO_2 nanocomposite The growth phase is critical in the synthesis of nanocomposite materials. For Cd-TiO_2 nanocomposite powder, the broad peak was located between 350 nm.

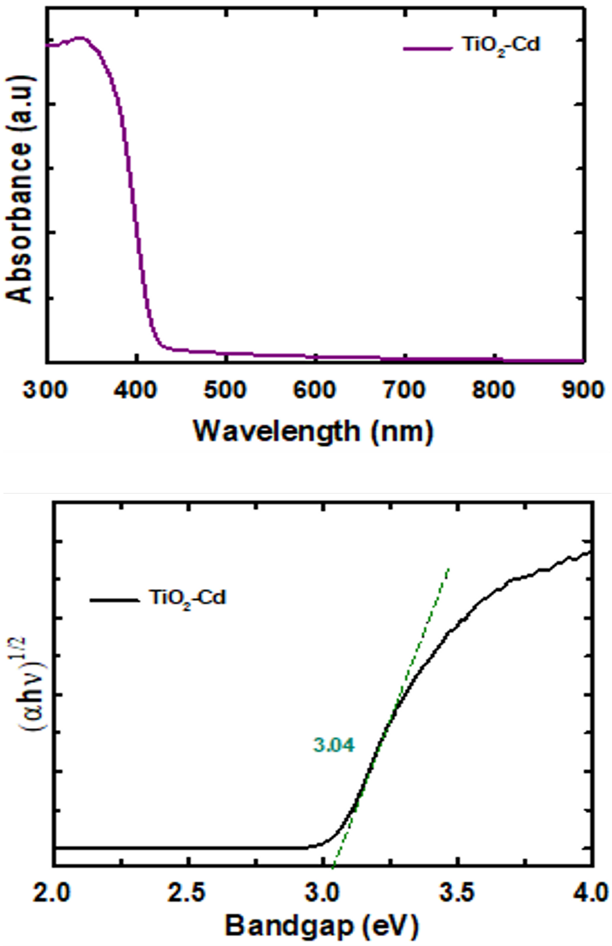

Figure 2: The UV image of Cd-TiO_2 nanocomposite

The absorbance of Cd-TiO_2 nanocomposite that was gradually increased after indicates gradual increase of nanocomposite. Finally, the result shows that the UV-visible absorption spectrum of Cd-TiO_2 nanocomposite shows an absorption onset at 350 nm (band gap = 3.04eV).

Fourier Transform Infrared Spectroscopy

From 4000 to 500cm^{-1}, several vibration bands of the Cd-TiO_2 Nanocomposite can be observed (Figure 3). The broad peak at around 3638cm^{-1} in the higher energy region can be attributed to the stretching vibrations band observed at the O-H bond in the carboxyl group (Zhu *et al.*, 2016).

The bands observed for the C-N bond at 1202cm^{-1} and 1126cm^{-1} correspond to the stretching vibrations of aliphatic and aromatic amines, respectively. The peak at 531 cm^{-1} corresponds to the anatase phase of TiO_2. The Ti–O stretching vibration and the Ti-O-Ti lattice are responsible for the 417cm^{-1} decrease in conduction elsewhere (Golobostanfard and Abdizadeh, 2013). The FTIR spectral results revealed possible interactions of the Cd-TiO_2

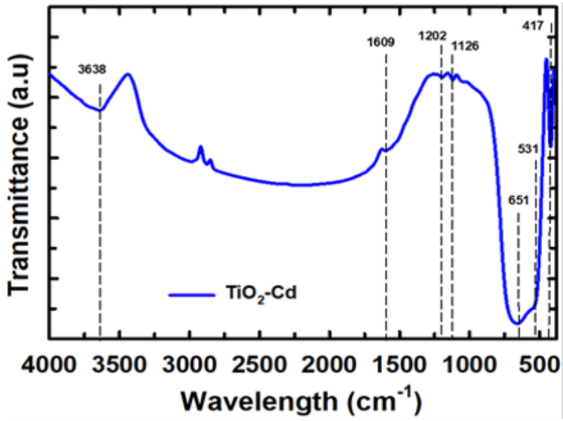

Figure 3: FTIR image of Cd-TiO_2 Nanocomposite

Nanocomposite, which could be responsible for the nanocomposite's stabilisation (Zhu *et al.*, 2016).

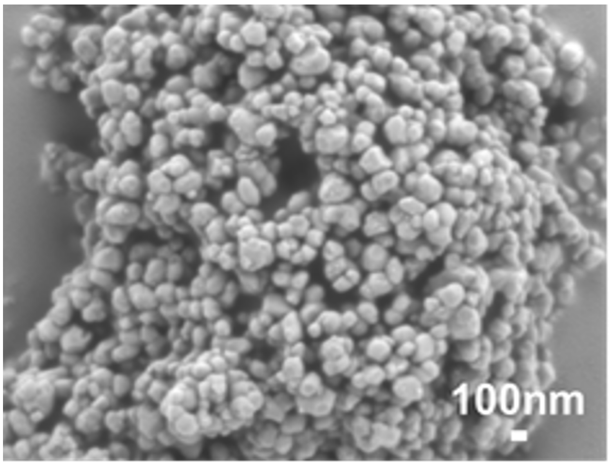

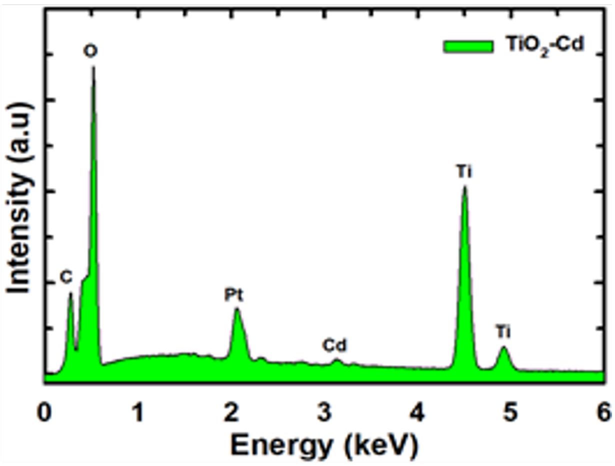

Figure 4: The SEM image of Cd-TiO_2 Nanocomposite

Scanning Electron Microscopy-EDAX

The morphological analysis of the synthesised Cd-TiO_2 Nanocomposite was learned using SEM. The SEM images of Cd-TiO_2 Nanocomposite are shown in Figure 4, and the average size of the Cd-TiO_2

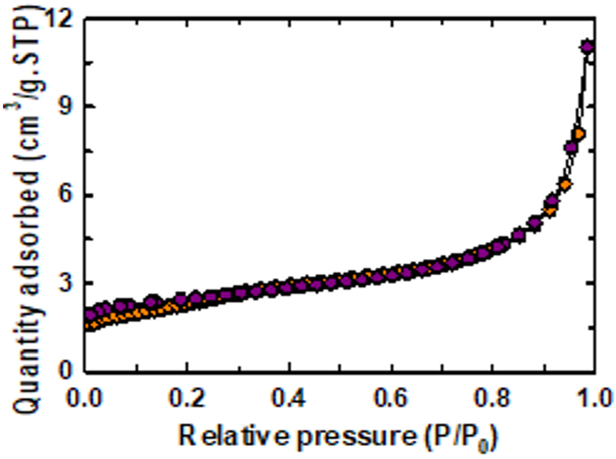

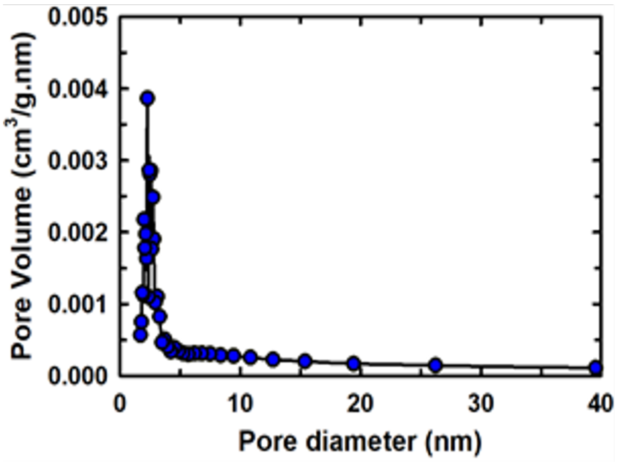

Figure 5: The BET image of Cd-TiO_2 Nanocomposite

Nanocomposite is determined to be in the range of 35nm. Cd-TiO_2 Nanocomposite shape such as spherical shape and then crystalline nature.

The purity of the synthesised Cd-TiO_2 Nanocomposite was confirmed by the energy dispersive X-ray (EDAX) spectra, which are shown in Figure 4 and Figure 5, respectively, and then C, O, Ti, Cd, and Pt elements are present in Cd-TiO_2 Nanocomposite. As shown in Figure 4, the weight percentage of Cd is 5.8 percent, Ti is 51.03 percent, C is 5.13 percent, and O is 31.75 percent in Cd-TiO_2 Nanocomposite. The EDAX spectra also confirm the doping in Cd nanocrystals. The absence of any additional impurity peaks in the spectra demonstrates the purity of the prepared nanocrystals.

BET Surface Area Analysis

The N_2 adsorption–desorption isotherms and BJH pore size distribution of Cd-TiO_2 nanocomposites are depicted in Figure 5. The N_2 adsorption–desorption isotherms of the as-prepared Cd-TiO_2 nanocomposites demonstration type IV characteristics, which is one of the main characteristics of

Figure 6: Antibacterial activity image of Cd-TiO_2 Nanocomposite

mesoporous materials. Major pore size distribution of Cd-TiO_2 nanocomposites is ranged from 2.24 nm.

The BET surface area of the prepared Cd-TiO_2 nanocomposites pore volume was 0.01cm^3/g. The surface area of Cd-TiO_2 nanocomposites is calculated to be 8.1 m2 g^{-1} built on the BET model. The surface area of BET and mesoporous structure improve the Photo generated electrons and holes toward contribute now photocatalytic activity and deliver more channels on behalf of water molecule to go through, which is important to complete high water and photo reduction efficacy (Zhang *et al.*, 2018).

Antibacterial Activity

The antibacterial activity of a synthesised Cd-TiO_2 nanocomposite (Das *et al.*, 2010) against Gramnegative bacteria was investigated using the well diffusion method (Das *et al.*, 2012, 2011, 2013).

As shown in Figure 6, a prepared solution of Cd-TiO_2 nanocomposite with various concentrations (such as 25, 50, 75, and 100 ml) is placed in the broth against Pseudomonas. In this case, the standard antibiotic ampicillin serves as a reference, while distilled water serves as a control.

The zone of inhibition (ZOI) on bacterial growth was observed and recorded after 24 hours of incubation, as shown in Figure 6. A measuring ruler was used to determine the diameter of the ZOI.

When tested against pathogens such as Pseudomonas, the Cd-TiO_2 nanocomposite demonstrated antibacterial activity (Figure 6).

The zone of minimum inhibition concentration was measured in 25ml at 20mm and 100ml at 30mm.

CONCLUSION

The Sol-Gel technique, we created a high purity bulk single phase Cd-TiO_2 nanocomposite powder. X-ray diffraction for the crystallite size is calculated and found to be Scherrer formula applied to the three highest peak such as 27.1°, 36.0°, 54.5° orientation which is the maximum reflection of the rhombohedral structure of Cd-TiO_2 nanocomposite. The particle size of Cd-TiO_2 nanocomposite in 35nm. The UV-visible absorption spectrum of Cd-TiO_2 nanocompositeshows an absorption onset at 350 nm (band gap = 3.04eV). The SEM image shows that the Cd-TiO_2 Nanocomposite shape such as spherical shape and then crystalline nature. The energy dispersive X-ray (EDAX) spectra confirmed the purity of the synthesised Cd-TiO_2 Nanocomposite, and then C, O, Ti, Cd, and Pt elements are present in Cd-TiO_2 Nanocomposite. In Cd-TiO_2 Nanocomposite, the weight percentage of Cd is 5.8 percent, Ti is 51.03 percent, C is 5.13 percent, and O is 31.75 percent. BET image shows that the major pore size distribution of Cd-TiO_2 nanocomposites is ranged from 2.24 nm. The BET surface area of the prepared Cd-TiO_2 nanocomposites pore volume was 0.01cm^3/g. The surface area of Cd-TiO_2 nanocomposites is calculated to be 8.1 m^2 g^{-1} built on the BET model. The Cd-TiO_2 nanocomposite showed that the antibacterial activity when tested against the pathogens only gram-negative bacteria such as *Pseudomonas*. The zone of minimum inhibition concentration was measured in a range of 20mm in 25μl and 30mm in 100μl.

Funding Support

The authors declare that they have no funding support for this study.

Conflict of Interest

The authors declare that there is no conflict of interest.

REFERENCES

Azam, A., Ahmed, A. S., Oves, M., Khan, M. S., Habib, S. S., Memic, A. 2012. Antimicrobial activity of metal oxide nanoparticles against Gram-positive and Gram-negative bacteria: a comparative study. *International Journal of Nanomedicine*, 7:6003–6009.

Chen, W., Sun, X., Weng, D. 2006. Morphology control of titanium oxides by tetramethylammonium cations in hydrothermal conditions. *Materials Letters*, 60(29-30):3477–3480.

Das, R., Gang, S., Nath, S. S. 2011. Preparation and Antibacterial Activity of Silver Nanoparticles. *Journal of Biomaterials and Nanobiotechnology*, 2(4):472–475.

Das, R., Gang, S., Nath, S. S., Bhattacharjee, R. 2012. Preparation of linoleic acid-capped silver nanoparticles and their antimicrobial effect. *IET Nanobiotechnology*, 6(2):81–85.

Das, R., Nath, S. S., Chakdar, D., Gope, G., Bhattacharjee, R. 2010. Synthesis of silver nanoparticles and their optical properties. *Journal of Experimental Nanoscience*, 5(4):357–362.

Das, R., Saha, M., Hussain, S. A., Nath, S. S. 2013. Silver Nanoparticles and their Antimicrobial Activity on a Few Bacteria. *BioNanoScience*, 3(1):67–72.

Demir, R., Okur, S., Şeker, M. 2012. Electrical Characterization of CdS Nanoparticles for Humidity Sensing Applications. *Industrial and Engineering Chemistry Research*, 51(8):3309–3313.

Dislich, H. 1993. Sol. Gel Technology for Thin Films, Fibers, Preforms, Electronics and Speciality Shapes. page 50. Edited by L. C. Klein (Noyes Publications, Prak Ridge, NJ).

Fades, B. D., Zelinski, B. J., Uhlmann, D. R. 1993. Ceramic. Films and Coatings. page 224. Edited by J. Wachtmann and JR. A. Haber (Noyes Publications, Park Ridge, NJ).

Giovanni, M., Tay, C. Y., Setyawati, M. I., Xie, J., Ong, C. N., Fan, R., Yue, J., Zhang, L., Leong, D. T. 2015. Toxicity profiling of water contextual zinc oxide, silver, and titanium dioxide nanoparticles in human oral and gastrointestinal cell systems. *Environmental Toxicology*, 30(12):1459–1469.

Golobostanfard, M. R., Abdizadeh, H. 2013. Effects of acid catalyst type on structural, morphological, and optoelectrical properties of spin-coated TiO2 thin film. *Physica B: Condensed Matter*, 413:40–46.

Han, Y., Li, G., Zhang, Z. 2006. Synthesis and optical properties of rutile TiO2 microspheres composed of radially aligned nanorods. *Journal of Crystal Growth*, 295(1):50–53.

Li, L., Yang, X., Gao, J., Tian, H., Zhao, J., Hagfeldt, A., Sun, L. 2011. Highly Efficient CdS Quantum Dot-Sensitized Solar Cells Based on a Modified Polysulfide Electrolyte. *Journal of the American Chemical Society*, 133(22):8458–8460.

Malarkodi, C., Chitra, K., Rajeshkumar, S., Gnanajobitha, G., Paulkumar, K., Vanaja, M., Annadurai, G. 2013. Novel eco-friendly synthesis of titanium oxide nanoparticles by using Planomicrobium sp. and its antimicrobial evaluation. *Der Pharmacia Sinica*, 4(3):59–66.

Pelaez, M., Nolan, N. T., Pillai, S. C., Seery, M. K., Falaras, P., Kontos, A. G., Dunlop, P. S. M., Hamilton, J. W. J., Byrne, J. A., O'Shea, K., Entezari, M. H., Dionysiou, D. D. 2012. A review on the visible light active titanium dioxide photocatalysts for environmental applications. *Applied Catalysis B: Environmental*, 125:331–349.

Pettit, R. B., Ashley, C. S., Reed, S. T., Brinker, C. J. 1993. Sol. Gel Technology for Thin Films, Fibers, Preforms, Electronics and Speciality Shapes. page 80. Edited by L. C. Klein, Noyes Publications, Prak Ridge, NJ.

Phani, A. R., Passacantando, M., Santucci, S. 2000. Synthesis and characterization of cadmium titanium oxide powders by sol-gel technique. *Journal of Materials Science*, 35(21):5295–5299.

Phani, A. R., Santucci, S., Nardo, S. D., Lozzi, L., Passacantando, M., Picozzi, P., Cantalini, C. 1998. Preparation and characterization of bulk ZnGa2O4. *Journal of Materials Science*, 33(15):3969–3973.

Qian, J., Yan, S., Xiao, Z. 2012. Electrochemical biosensor based on CdS nanostructure surfaces. *Journal of Colloid and Interface Science*, 366(1):130–134.

Rzigalinski, B. A., Strobl, J. S. 2009. Cadmium-containing nanoparticles: Perspectives on pharmacology and toxicology of quantum dots. *Toxicology and Applied Pharmacology*, 238(3):280–288.

Samuel, V., Pasricha, R., Ravi, V. 2005. Synthesis of nanocrystalline rutile. *Ceramics International*, 31(4):555–557.

Tabatabaee, M., Baziari, P., Nasirizadeh, N., Dehghanizadeh, H. 2013. Synthesis of CdS Nanoparticles by Sonochemical Reaction Using Thioasetamide as S2— Reservoir and in the Presence of a Neutral Surfactant, Dyeing of Cotton Fabric and Study of Antibacterial Effect on Cotton Fabric. *Advanced Materials Research* , 622:851–854.

Tsutomu, U., Tetsuya, Y., Sigeru, T., Keisuke, A. 2003. Visible Light-Induced Degradation of Methylene Blue on S-doped TiO2. *Chemistry Letters*, 32(4):330–331.

Vanaja, M., Rajeshkumar, S., Paulkumar, K., Gnanajobitha, G., Malarkodi, C., Annadurai, G. 2013. Phytosynthesis and characterization of silver nanoparticles using stem extract of Coleus aromaticus. *International Journal of Materials and Biomaterials Applications*, 3(1):1–4.

Zare, M., Namratha, K., Byrappa, K., Surendra, D. M., Yallappa, S., Hungund, B. 2018. Surfactant assisted solvothermal synthesis of ZnO nanoparticles and study of their antimicrobial and antioxidant properties. *Journal of Materials Science and Technology*, 34(6):1035–1043.

Zhang, H., Wang, X., Li, N., Xia, J., Meng, Q., Ding, J., Lu, J. 2018. Synthesis and characterization of TiO2/graphene oxide nanocomposites for photoreduction of heavy metal ions in reverse osmosis concentrate. *RSC Advances*, 8(60):34241–34251.

Zhu, X., Kumari, D., Huang, M., Achal, V. 2016. Biosynthesis of CdS nanoparticles through microbial induced calcite precipitation. *Materials and Design*, 98:209–214.